16th World Conference on Earthquake Engineering, 16WCEE 2017
Santiago Chile, January 9th to 13th 2017
Paper N° 4510
Registration Code: S-P1464657184

EARTHQUAKE RESPONSE EVALUATION WITH A NEW HYSTERETIC MODEL

A. Bertero[1], T. N. Do[2], F. C. Filippou[3]

[1] Universidad de Buenos Aires, abertero@fi.uba.ar
[2] University of California, Berkeley, tdongoc@berkeley.edu
[3] University of California, Berkeley, filippou@berkeley.edu

Abstract

This study addresses an acute need in the damage assessment of existing and new structures within the framework of performance based earthquake engineering: the ability to simulate in consistent, accurate and numerically robust fashion the damage evolution of structural components and systems under the effect of moderate and strong earthquake ground motions. The first part of the paper describes a new damage model for the response simulation of structural components with strength and stiffness degradation under cyclic loading condition. The second part of the study uses the damage model to evaluate the response of structural systems under two different suites of ground motions. Idealized as single-degree-of-freedom oscillators, two systems with very distinct hysteretic behaviors are selected for illustration: ductile and limited-ductility reinforced concrete frames. The performance evaluation focuses on strength loss and residual displacements, two measures that are considered critical for resilience assessment, identifying threshold values that would imply intolerable structural damage and economic loss. This analysis showcases the ability of the new hysteretic model to represent different degrading responses and to describe structural performance and post-earthquake condition through the model's damage variable. Additionally, the large amount of generated data is used to investigate the evolution of these measures in each system, as related to other parameters such as the intensity of the ground motion, the extreme displacements, and the cyclic degradation.

Keywords: Hysteretic Model, Strength and Stiffness Deterioration, Damage Measure, Resilience, Nonlinear Seismic Response

1. Introduction

Over the last several decades, the engineering community is continuously reminded of the lack of resilience in the built-environment by earthquakes and other natural disasters, that causes intolerable structural damage, economic loss, and, oftentimes, significant loss of life. In the framework of performance-based earthquake engineering, it is, therefore, critical to establish an accurate, consistent, and efficient analytical model for the simulation and damage assessment of structures. Do and Filippou [1] have recently proposed a hysteretic model that addresses this need with its ability to describe the degrading hysteretic response on the basis of a continuous damage variable.

The proposed model is used in this study to simulate the degrading response of structural systems under strong ground motions. The systems are analyzed as single-degree-of-freedom (SDOF) oscillators with hysteretic behaviors that follow the recommendations in FEMA P-440A [2]. Modeling multi-story buildings as a SDOF with a backbone curve that mimics its static pushover response is a widely used approach in the literature. While the response of a real structure is much more complex, several studies have stated that the results and conclusions from the simple model can be extended to multi-degree-of-freedom systems. The comprehensive literature search in FEMA P-440A presents many of these studies. In this paper, the systems are subjected to Incremental Dynamic Analysis [3] for two different suites of ground motions to assess the evolution of deterioration and permanent displacements, two measures that are considered critical to control for minimizing post-earthquake disruption and economic losses. The earthquake response evaluation conducted in this study also demonstrates the capabilities of the model, as related to its numerical efficiency and robustness, and its ability to describe very different hysteretic behaviors.

2. A New Hysteretic Model

The recent hysteretic damage model by Do and Filippou [1] is adopted in the present study. The formulation is based on the concepts of damage mechanics and relates any two work-conjugate variables *s*-*e*, such as force-displacement, moment-rotation, moment-curvature, or stress-strain hysteretic relations. Fig. 1 illustrates the interplay of the three independent components of the model: first the backbone relation between deformation e and effective force $\bar{s}$ is defined, as represented by the long dash line in the figure. Behind the scenes the damage loading function describes the condition of damage growth in terms of internal energy dissipation. Finally, a damage evolution law relates the value of the damage loading function to the damage variable d, which is then used to reduce the effective force $\bar{s}$ to the true force s and the effective unloading stiffness $\bar{E}$ to the true unloading stiffness E.

To describe the "effective" force-deformation relation this study adopts the bilinear model with elastic unloading and a bilinear reloading path in Fig. 2 that represents either the "pinching" or the Bauschinger effect of the hysteretic relation. The continuous strength and stiffness degradation depends on the evolution of a damage variable d on the basis of a damage loading function and an evolution law. The loading function defines the condition of damage growth in terms of an energy variable ψ, such that further damage takes place when the energy variable exceeds the corresponding previous energy threshold. To exhibit different response under positive and negative forces, the model separates the variables and distinguishes the damage evolution between positive and negative force states. The energy variables $\psi^{\pm}$ depend on the extreme deformations (e_{min}, e_{max}) and the positive and negative energy dissipations, ψ_t and ψ_c, which are defined by the integral of the effective forces, $\bar{s}^{+}$ and $\bar{s}^{-}$, with the deformation increment de. The contributions to the energy variables $\psi^{\pm}$ from the energy dissipation under positive and negative forces, ψ_t and ψ_c, are weighed differently to capture the coupling effect on the damage in opposite directions. The model also assigns different weights to the energy dissipation increments to distinguish the primary half cycles when the deformations exceed the previous extreme values from the follower half cycles when the deformations are within the extreme values.

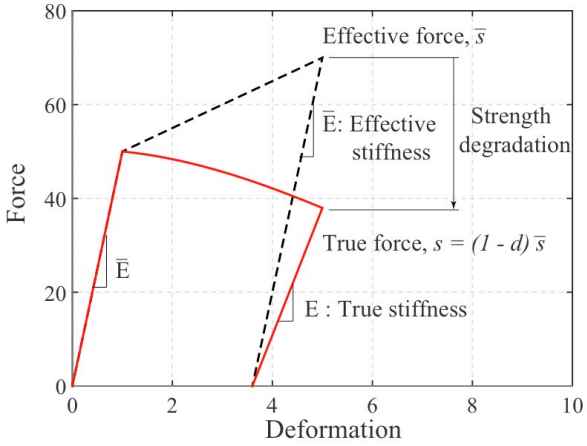

Fig. 1: Relation between effective and true response

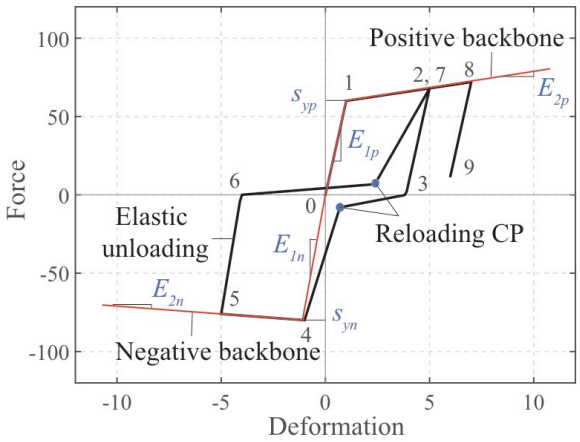

Fig. 2: Bilinear Hysteretic Model

The damage evolution law follows a cumulative distribution function (CDF) to describe the damage variables $d^{\pm}$ in terms of the energy variables $\psi^{\pm}$. The damage variables are monotonically increasing and range from $d = 0$ in the virgin material to $d = 1$ at complete loss of strength. After determining the damage variable $d^{\pm}$, the true force s is determined with the following linear combination of the positive and negative effective force, $\bar{s}^{+}$ and $\bar{s}^{-}$:

$$s = (1 - d^{+})\bar{s}^{+} + (1 - d^{-})\bar{s}^{-} \tag{1}$$

Fig. 3a shows the force-deformation relation of the damage model under a sample cyclic deformation history. The hysteretic damage model accommodates both types of degradation in FEMA P-440A: the cyclic and in-cycle degradation [2]. The former is evident in the strength reduction between load point (LP) 8 and 12. The latter is evident in the strength deterioration between LP 2 and 3, LP 16 and 17. Fig. 3b shows the evolution of the positive damage variable d^{+} for the load history in Fig. 3a, noting that the negative damage variable follows a similar trend due to the symmetric deformation history. The rate of increase of the damage variable is highest when the deformation exceeds the maximum previous values, such as between LP 2 and 3, LP 16 and 17. The damage variable increases at a lower rate under positive deformation not exceeding the previous maximum value, as in the case between LP 7 and 8, LP 11 and 12, LP 15 and 16. The damage variable also increases under negative deformations due to the damage coupling effect, such as between LP 5 and 6, LP 19 and 20.

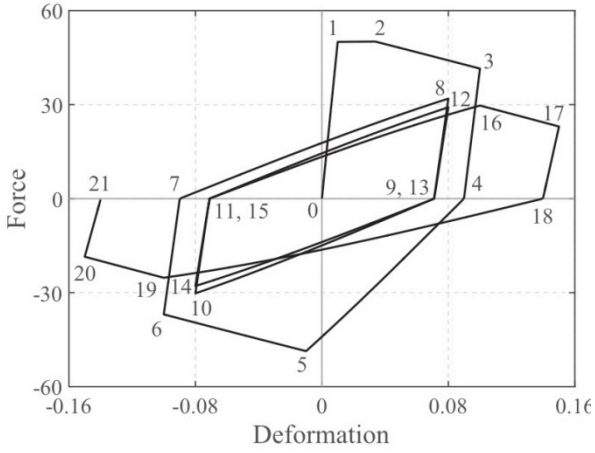

Fig. 3a: Sample cyclic force-deformation response

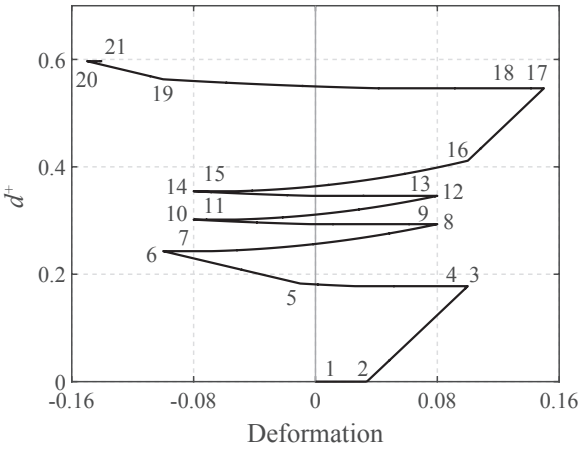

Fig. 3b: Evolution of the positive damage variable d^{+}

3. Degrading Hysteretic Behavior of Systems

This section uses the damage model for the response simulation of two structural systems to showcase the ability of the model to represent different degrading hysteretic behaviors. The two systems used for testing the model's capabilities in this study are: a ductile reinforced concrete frame system, subsequently referred to as model M1, and a limited ductility reinforced concrete frame system, referred to as model M2. The selected systems are two cases among the hysteretic behaviors of structural systems with strength and stiffness degradation in the framework of FEMA P-440A Recommendations [2]. The subsequent paragraphs describe the two systems and explain how the model parameters are calibrated to match the experimental results. However, it is worth pointing out that the intention is not to represent exactly the behavior of any particular component, but rather to capture the major characteristics of the response of each system.

3.1. Model M1: Ductile Reinforced Concrete Frame

Model M1 represents the behavior of ductile reinforced concrete structures, such as special moment frames designed per ACI requirements for high-seismicity areas. Its hysteretic behavior falls into the "ductile moment frame systems" category as classified in the FEMA P-440A Recommendations. Results from an experimental test by Saatcioglu and Grira [4] on a ductile column representative of the system are presented in Fig. 4a. The numerical simulation is characterized by a bilinear hysteretic backbone curve for the effective force-deformation relation that yields at a drift of 1% and has positive post-yielding slope. No pinching effects are present. It is assumed that damage starts to accumulate immediately after yielding occurs, but with an intensity that will allow for a ductile response. Fig. 4b compares the force-deformation relation of the true and effective spaces to illustrate the continuous strength and stiffness degradation due to the evolution of the damage variables. Additionally, the figure shows the monotonic curve recommended in FEMA P-440A for a system of these characteristics. The comparison between figures (a) and (b) shows the good agreement obtained between the numerical solution and the experimental results.

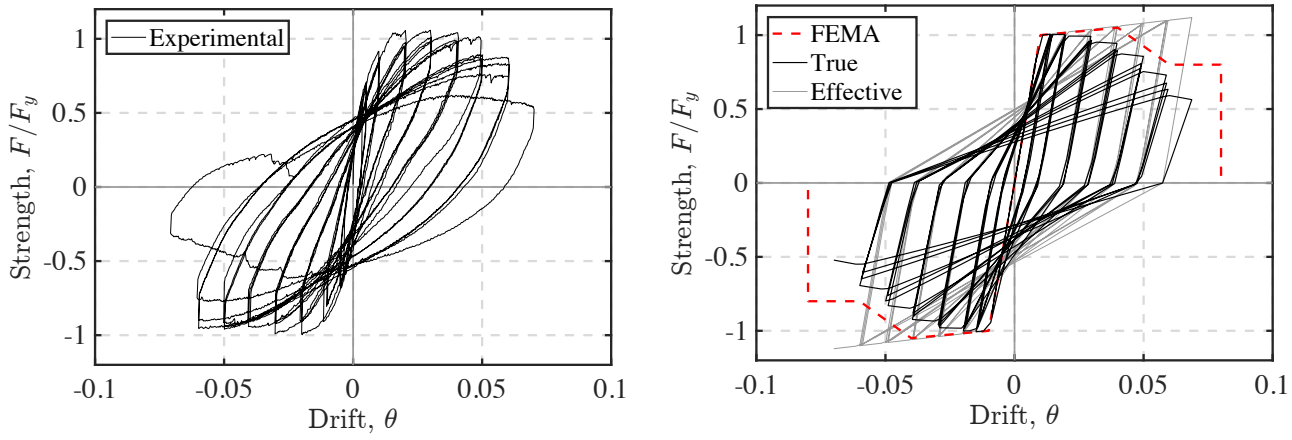

(a) Saatcioglu and Grira, BG-6

(b) Model M1

Fig. 4: Model M1 and comparison with experimental test

3.2. Model M2: Limited Ductility Moment Frame

Model M2 represents the behavior of limited ductility moment resisting frames in buildings. Systems with this type of behavior include older reinforced concrete frames not designed for seismic loads, which can be be lightly reinforced and may have inadequate joint reinforcement or concrete confinement. An example of a member with this type of behavior is the shear-critical reinforced concrete column tested by Sezen and Moehle [5] presented in Fig. 5a. To capture the inadequate detailing for ductility, the reloading behavior represents the pinching effect of the hysteretic behavior. As in model M1, a bilinear backbone curve is used for the effect force-deformation relation with yield drift ratio equal to 1%. In this case, damage initiates at a drift close to 2%, and accumulates

faster in the onset of damage than later in the response. Cyclic deterioration and damage coupling are more intense in this case than in model M1. The resulting force-deformation relation is presented in Fig. 5b, together with the effective response and the monotonic backbone recommended by FEMA for this class of system. Again, good agreement is obtained between the numerical simulation and the experimental results.

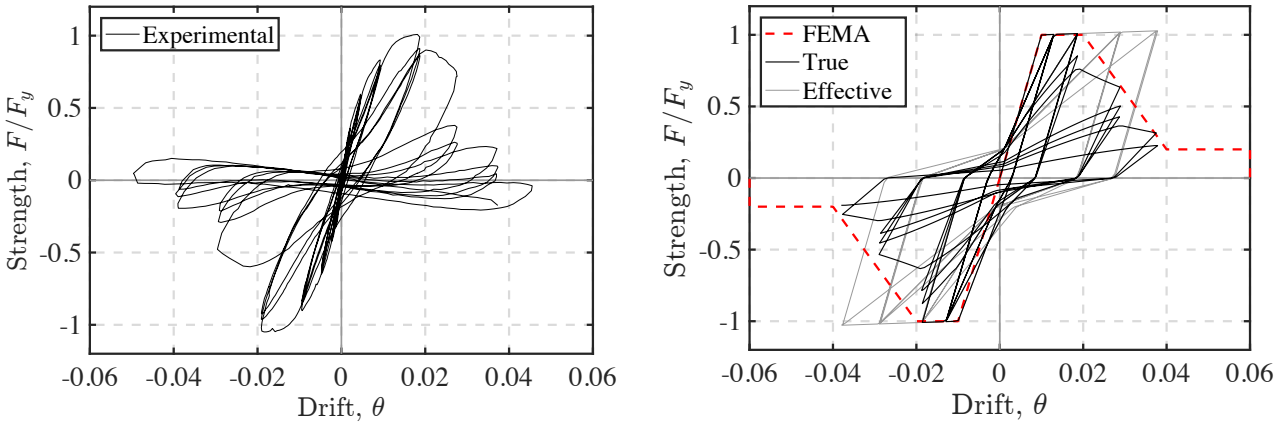

(a) Sezen and Moehle, No. 1 (b) Model M2

Fig. 5: Model M2 and comparison with experimental test

3.2. Summary of model parameters

A detailed description of the required parameters of the damage model can be found in [1]. Table 1 summarizes the parameters for the response simulation of models M1 and M2 in this study. The top 4 rows of the table contain the parameters that describe the force-deformation relation in the effective space. The backbone curve for the bilinear hysteretic model in Fig. 2 requires 3 parameters: the yield strength s_y, the initial modulus E_1, and the post-yield modulus E_2. Furthermore, the bilinear hysteretic model has two more parameters p_x and p_y which are the relative coordinates of the control point for the bilinear reloading branch in Fig. 2. In model M1, the selection $p_x = p_y$ with any values between 0 and 1 results in a linear reloading branch from the point of complete unloading to the maximum previous deformation of opposite force to the force at unloading initiation. In model M2, the condition $0 \leq p_y < p_x \leq 1$ describes the pinching behavior in the reloading response due to sliding, slip, and shear deformation [1].

The model parameters that control the damage evolution are the threshold damage parameter C_{d0}, the limit damage parameter C_{d1}, two parameters of the damage evolution law d_{p1} and d_{p2}, the damage coupling coefficient C_{cd}, and the weight coefficient C_{wc} for cyclic degradation. The threshold parameter $C_{d0} = 1$ in model M1 represents the onset of strength reduction upon yielding of reinforcements. The threshold $C_{d0} = 5$ in model M2 delays the onset of damage and captures the yield plateau. The selection of the limit coefficient C_{d1} reflects the displacement ductility capacity of the two models, with $C_{d1} = 40$ in model M2 representing a relatively lower displacement ductility than model M1 with $C_{d1} = 80$. The different values for the parameters d_{p1} and d_{p2} distinguish the different damage evolution between the two models. The selection of the value of 0.6 for the damage parameter d_{p2} in combination with the value of 3 for the damage parameter d_{p1} is meant to capture the rapid strength deterioration following the onset of damage of model M2. In contrast, the deterioration in the response of model M1 accumulates at a higher displacement by the selection of a lower value for $d_{p1} = 1.2$ and a value greater than 1 for d_{p2}, with $d_{p2} = 1.5$. The level of damage coupling and cyclic degradation is reflected in the damage coupling coefficient C_{cd} and the cyclic degradation coefficient C_{wc}. Higher values of C_{cd} and C_{wc} describe a more pronounced damage interaction under positive and negative forces and more rapid cyclic degradation in the response of M2 relative to M1. In this study, the force-deformation relation is assumed symmetric which results in the same parameters describing the response under positive and negative forces.

This study does not attempt to optimize the parameters for best fit. Better agreement with the experimental results is certainly possible through a formal parameter identification algorithm, which is left for future study.

Table 1: Parameters for the response simulation of model M1 and M2 expressed in terms of s_y

Parameter		**Model M1**	**Model M2**
E_1	elastic stiffness	$100\,s_y$	$100\,s_y$
E_2	post-yield stiffness	$2\,s_y$	$2\,s_y$
p_x,	reloading x-coordinate	0	0.5
p_y,	reloading y-coordinate	0	0.2
C_{d0},	threshold coefficient	1	5
C_{d1},	limit coefficient	80	40
d_{p1},	first damage parameter	1.2	3
d_{p2},	second damage parameter	1.5	0.6
C_{cd},	damage coupling coefficient	0.35	0.45
C_{wc},	cyclic degradation coefficient	0.15	0.45

4. Earthquake Response Evaluation: Methodology

The two models of the previous section for describing the hysteretic behavior of ductile and limited ductility reinforced concrete frames are used to evaluate the response of structural systems during strong ground motions. The subsequent discussion presents the methodology and measures adopted in this study for performance assessment.

4.1. Damage measures

Many studies on the behavior of multi-story buildings under strong ground motions focus on the structural response at or near collapse. However, with the growing demand for earthquake-resilient structures, it is becoming critical to evaluate the structural performance at other limit states prior to collapse that still result in significant economic losses. Data taken from the Loma Prieta and Northridge Earthquakes show that per each building that collapsed, 13 others were seriously damaged and left unsafe or prohibited to occupy [6]. These conditions lead to high or total economic losses even if collapse is prevented due to either prolonged downtime or repairs becoming uneconomical.

For evaluating the response of the systems, this study selects the two key parameters that need to be controlled to minimize post-earthquake disruption as the "damage measures": (a) the strength loss of the structural system, and (b) the permanent displacements. Guidelines currently widely used in practice recommend maximum allowable values for these two measures. Regarding strength loss, the Tall Building Initiative Guidelines [7] recommend that the loss in lateral story resistance at maximum drift should not be more than about 20% of the original resistance. Similarly, to protect the building against unacceptable post-earthquake deformations that will likely cause condemnation or excessive downtime for a building, this Guideline limits residual story drifts to 1%. FEMA P-58 [8] proposes a repair fragility in which this value is assumed to correspond to a 50% probability of the building becoming irreparable. Following these recommendations, the threshold values adopted in this study up to which structural response is assessed are

$$d = 0.20 \tag{2a}$$

$$\theta_{res} = 1\% \tag{2b}$$

where d is the damage variable and θ_{res} the residual drift ratio. The ability to directly relate the degrading hysteretic behavior to the damage variable d makes the damage model in Section 2 convenient and suitable for the evaluation and assessment of the two performance conditions.

4.2. Incremental Dynamic Analysis

Incremental Dynamic Analysis [3] is performed until the conditions in Equation (2) are met. To construct the IDA curves, the strength reduction coefficient $R_y = S_a(T) / S_{ay}(T)$ is adopted as a normalized Intensity Measure, where $S_a(T)$ is the spectral acceleration at the fundamental period of vibration of the SDOF, and $S_{ay}(T)$ is the intensity that causes first yield to occur in the system. The IDA curves are plotted against the peak transient drift ratio θ.

IDA curves vary significantly from one ground motion to the other. Because of this variability, known as record-to-record variability, the response of a system due to any one record is highly uncertain. For this reason, statistical information on the response due to a suite of ground motions is required to quantify the median and dispersion of the behavior of a structure. Two sets of motions are considered in this study, which are similar to those selected in FEMA documents P-695 [9] and P-440A.

The first one, referred to as the "Far-Field" record set, includes 21 ground motion records from sites located at distances greater than or equal to 10km from fault rupture. The other set includes 14 records of ground motions with pulses recorded at sites less than 10km from fault rupture, and is referred to as the "Near-Field" record set. In both cases, only the first component of the record pairs adopted in the FEMA documents was considered. The average significant durations, defined as the time interval between the accumulation of 5% and 95% of ground motion energy, are 16 seconds and 13.1 seconds, respectively. The ground motion energy is given by the Arias Intensity. Fig. 6 shows the individual and median 5% damped elastic response spectrums corresponding to each set, normalized by their respective peak ground accelerations (PGA).

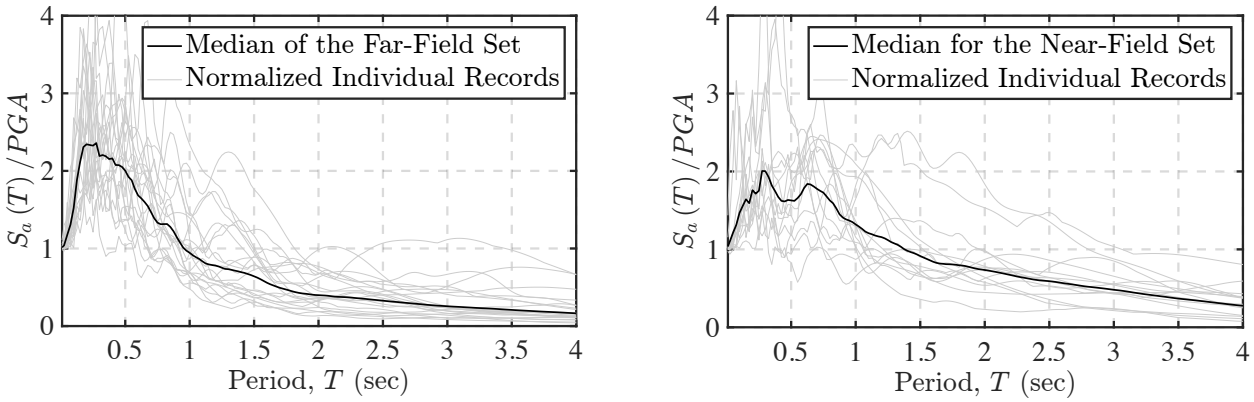

Fig. 6: Elastic response spectrum for the Far-Field (left) and Near-Field (right) sets

Both systems of Section 3 are tuned to three different natural periods, resulting in a total of 12 different cases (as each system-period pair is subjected to 2 suites of ground motions). In each case, the result of the analyses is a family of IDA curves. As an example, Fig. 7 shows the results for model M1 with a period of T = 1sec and subjected to the Far-Field set. After identifying in each curve the points at which the conditions in Equation (2) are first met, the probability density functions corresponding to these conditions are determined by fitting the data to a log-normal distribution. As shown in the figure, these functions can be expressed in terms of either an intensity or a damage measure, in this case R_y and θ, respectively.

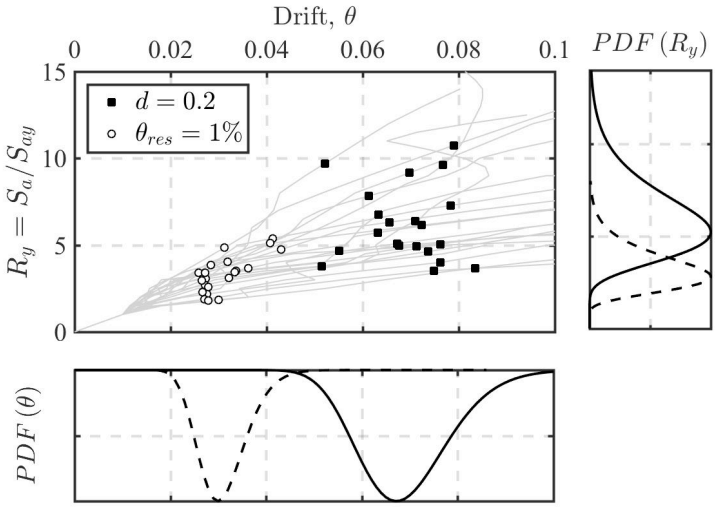

Fig. 7: Probability Density Functions (PDF) based on IDA curves

5. Earthquake Response Evaluation: Results

This section presents the results from the earthquake response evaluation of the degrading SDOF systems. In total, more than 3,000 nonlinear response analyses were conducted. A constant damping coefficient based on the initial stiffness and a damping ratio $\zeta = 2.5\%$ was considered. To account for nonlinear geometry effects, a linear elastic element with negative stiffness $K_{P\Delta} = -0.018\,TK_{el}$ is added in parallel with the damage model, where T is the natural period and K_{el} the elastic stiffness of the undegraded system. This value is representative of the PΔ effects in stiff structures, as adopted in previous studies [10].

5.1. Nonlinear geometry effects

The inclusion of nonlinear geometry effects in the analysis is justified in this section. Fig. 8 compares the results for model M2 with a period of 1sec and subjected to the Far-Field set. Clearly, while the maximum residual drift condition is significantly affected by nonlinear geometry effects (shown by the fact that the condition $\theta_{res} = 1\%$ is reached at lower intensities and drifts in (b) than in (a)), their influence in strength deterioration reaching a maximum value of 20% is almost negligible. Similar observations can be derived from the analysis of model M1. Given the importance that residual drifts play in loss estimation and resilience assessment, the inclusion of nonlinear geometry effects should not be omitted in the numerical model.

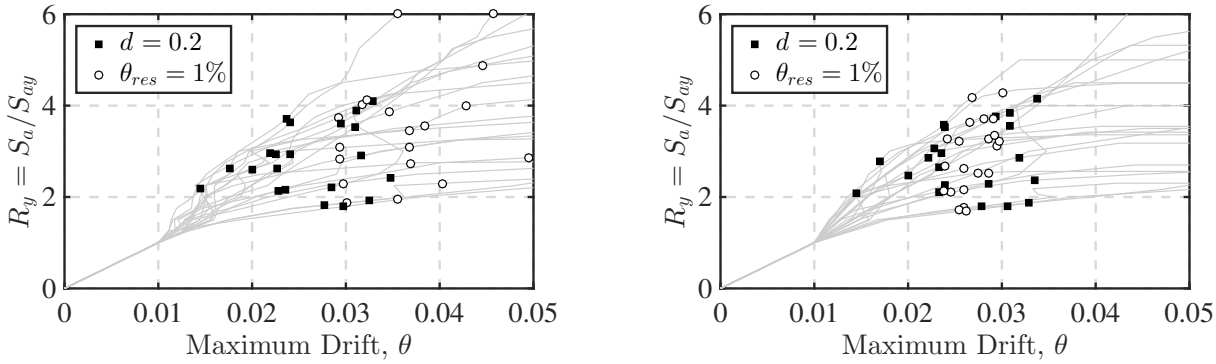

(a) Without PΔ effects

(b) Including PΔ effects ($K_{P\Delta} = -0.018\,TK_{el}$)

Fig. 8: Effect of nonlinear geometry in the response of model M2 (T = 1sec) subjected to the Far-Field set

5.2. Effect of ductility capacity

By repeating the procedure presented in Fig. 7 and integrating the probability density functions, the fragility curves corresponding to the conditions in Equation (2) are obtained. These are presented in Fig. 9 and Fig. 10 for models M1 and M2. In each figure, the solid and dash lines give the probability of exceeding the conditions in Equations (2a) and (2b), respectively. Fig. 9a and Fig. 10a express this probability in terms of the intensity measure R_y, and Fig. 9b and Fig. 10b do the same in terms of the maximum drift θ. The 6 pairs of lines in each figure correspond to the 6 cases being considered in each model (2 suites of ground motions and 3 periods).

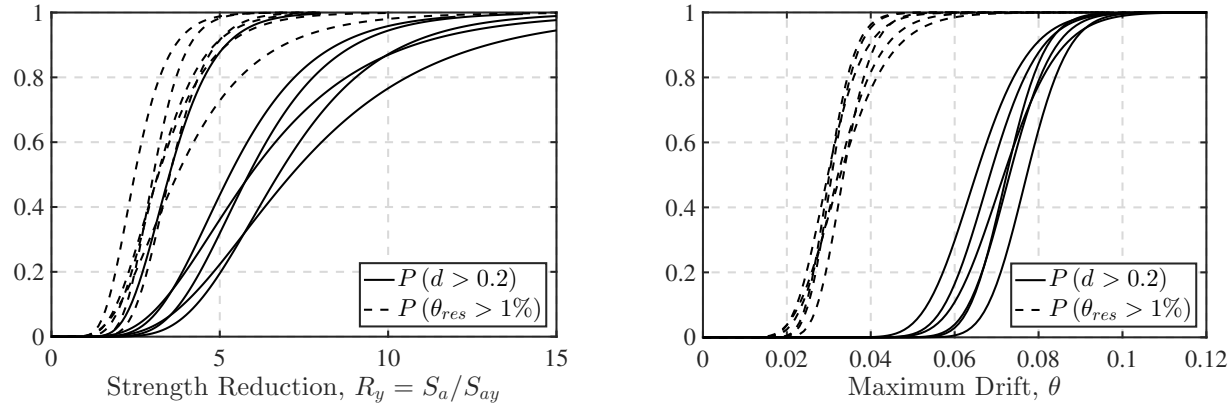

Fig. 9: Fragility curves for Model M1

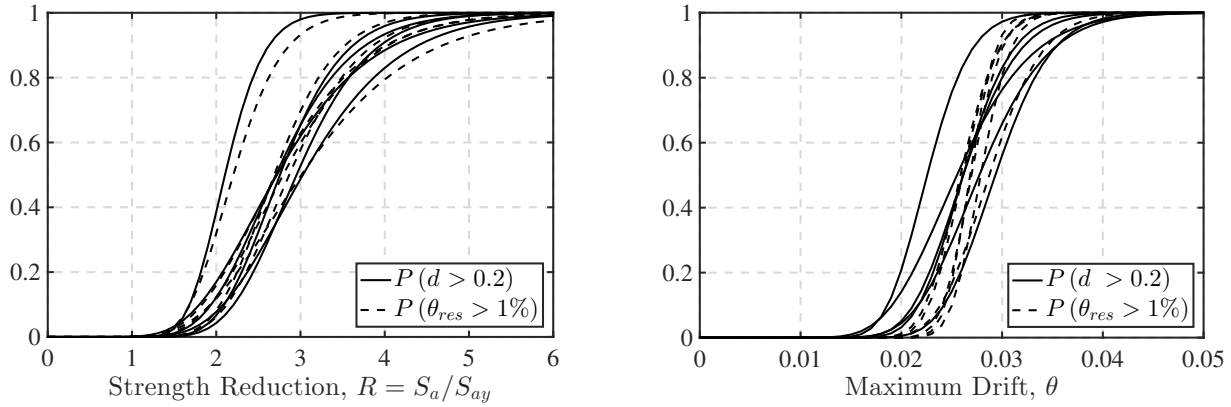

Fig. 10: Fragility curves for Model M2

Without distinguishing between the corresponding cases, several observations can be made from these figures. First, it is clear from Fig. 9 that in the ductile system the maximum residual drift condition is always reached before the strength reduction condition becomes significant. However, the same trend is not observed in the limited-ductility system M2, as implied by the fact that curves corresponding to reaching the conditions in Equation (2) are superimposed in Fig. 10. Given the repair fragility presented in FEMA P-58, this observation confirms that the impact of residual displacements in the total economic loss estimation should be higher in ductile structures than in non-ductile structures, as concluded in previous studies [11]. Focusing just on residual displacements, it is also observed that the R_y values that lead to a 50% probability of residual drifts being greater than 1% are in the same order of magnitude in both ductile and non-ductile systems. This second observation helps to illustrate the fact that designing ductile structures for collapse prevention is necessary, but not sufficient to minimize post-earthquake disruption due to intermediate limit states.

Fig. 11 shows the average standard deviations of the log-normal distributions presented above. The dispersion is always smaller when the fragilities are plotted as function of maximum drift rather than to the normalized measure for intensity R_y, suggesting that both strength loss and residual drift are strongly related to

the maximum displacement and less affected by record-to-record variability. This observation is confirmed by the results presented in Fig. 12, which show the relation between the two damage measures and the peak transient drift for each of 3,000 nonlinear response analyses in this study. Again, no distinction is made between the 6 cases corresponding to each model, meaning that each group of dots contains data from both the Far-Field and Near-Field sets, and for the three periods evaluated. Evidently, while the relation between the damage variable d and the peak transient drifts θ varies dramatically depending on the ductility capacity of the system (Fig. 12a), the relation between residual and peak transient drifts is independent of this property (Fig. 12b). The fact that the correlation between d and θ is so strongly related with the ductility capacity, regardless of other properties of the system or the ground motions, indicates that the influence of cyclic degradation and energy dissipation is of secondary importance in damage evolution related to extreme deformation. This matter is further discussed in the next section.

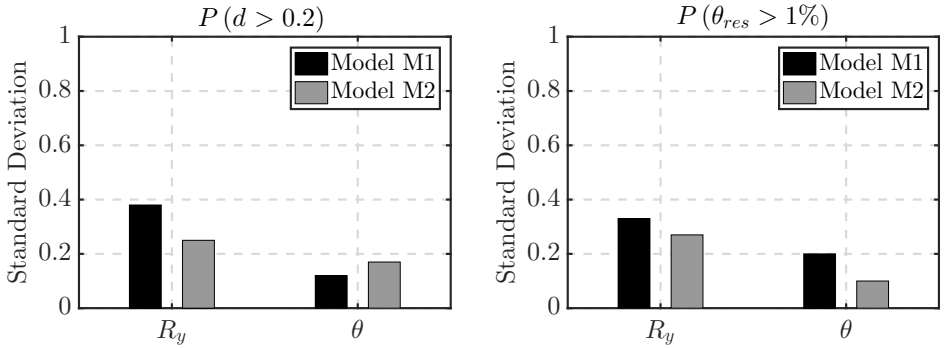

Fig. 11: Average dispersion for the conditions in Equation (1)

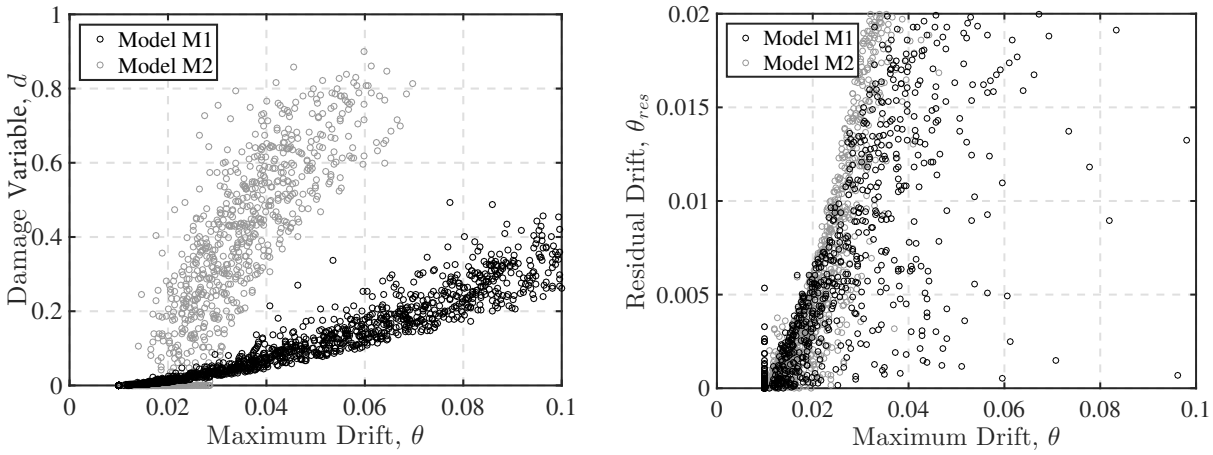

Fig. 12: Results from more than 3,000 nonlinear response analyses

5.2. Effect of cyclic degradation

Initial natural period and duration of the ground motion influence significantly the number of cycles of loading to which the structure will be subjected during an earthquake. Thus, the effects of cyclic degradation can be investigated by taking the results presented in Fig. 12a and distinguishing between the 6 cases considered in this study. Fig. 13 shows the results for model M2. The linear regressions of the damage variable as a function of maximum displacements corresponding to the different periods and ground motions sets are presented in Fig. 13a and Fig. 13b, respectively. The effect of cyclic degradation on the maximum displacements is out of the scope of the study. From the first figure, it is noticed that damage increases faster at smaller periods when compared to the peak transient drift. This is an expected result that is well captured by the model, as for a given record, a stiffer structure will be subjected to more cycles of loading and consequently it will be more affected by cyclic degradation. A similar conclusion can be derived by comparing the responses of model M2 to the Far-

Field (FF) and Near-Field (NF) sets. Fig. 13b indicates that for the same peak transient drift, the damage variable is larger for distant events, which force the structure to dissipate energy in more cycles of loading than those presenting one strong pulse (the average significant duration of the Far-Field set is 22% higher than the same for the Near-Field set). The same observations can be made analyzing the response of model M1, however the fact that cyclic degradation is larger in M2 accentuates these effects.

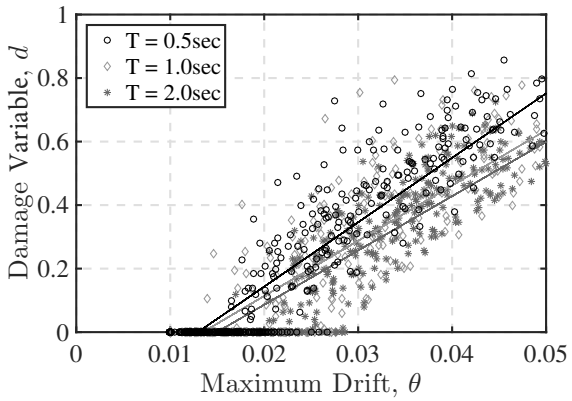

(a) Effect of Period

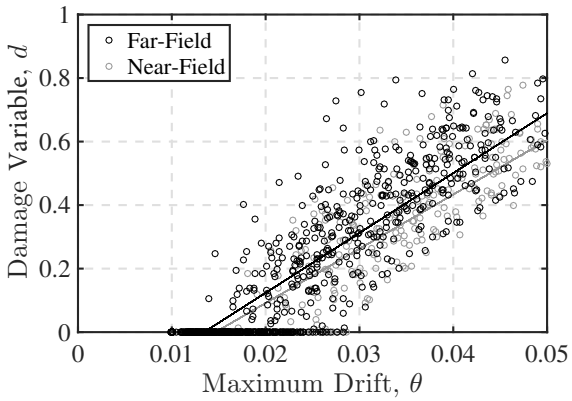

(a) Effect of directivity

Fig. 13: Results for the analysis corresponding to the model M2.

6. Concluding Remarks

The assessment of structural resilience imposes an increasing demand for new models that can reliably predict the response and damage of structures during strong ground motions. Do and Filippou recently developed a new hysteretic damage model for the response simulation of structural components with strength and stiffness deterioration under cyclic loading. It describes the degrading hysteretic response on the basis of a continuous damage variable.

The model is adopted in this study for the response simulation of two distinct structural systems to showcase its ability to represent different degrading hysteretic behaviors. The monotonically increasing damage variable of the model directly relates the degrading force-deformation response with the progressive damage state of the system. Although this study focuses on reinforced concrete structures, the flexibility of the damage evolution law and the fact that any type of hysteretic behavior can be considered for the constitutive model in the effective space allow for the response description of a wide spectrum of structural systems.

Strength loss and residual displacements are the two measures of interest in this study, as these are identified as the critical parameters that need to be controlled to assess the resilience of a system. The analyses for the different structural systems and suites of ground motion records result in a large collection of data. The most significant observations extracted from them are listed below:

- Damage and residual drifts primarily depend on the ductility demand, and thus, not affected by record-to-record variability as other measures are.
    - The relation between damage and ductility demand varies dramatically with the ductility capacity of the system. The very distinctive evolution trends obtained for each system, without consideration of directivity or period, show that the effect of cyclic degradation, while meaningful, is of secondary importance relative to extreme deformation.
    - In contrast, the relation between residual drifts and ductility demand is independent of the ductility capacity of the system, but strongly influenced by nonlinear geometry effects.
- Several guidelines intend to control damage indirectly by limiting maximum drifts. For example, the Tall Building Initiative Guidelines [7] limit peak transient drifts to 3% based on general consensus that up to this value well detailed structures will perform well without significant strength loss. This assumption is

confirmed in this study. According to the response analyses conducted for the ductile system M1, the strength loss corresponding to this drift threshold are on the order of 5%. However, for model M2 the expected strength loss for that same ductility demand is greater than 30%.

- On the other hand, drifts and intensities for which residual displacements become unacceptable are very similar in both cases. As a consequence, the impact of losses due to permanent displacements in total losses is higher in ductile structures than in non-ductile structures.

From the evaluation of the earthquake response, it is concluded that the model offers a descriptive measure of the performance of the structure and its post-earthquake condition, particularly through its damage variable, which explicitly defines the strength and stiffness deterioration of the system. Because of its consistent and numerically robust formulation, the model strikes a balance between accuracy and numerical efficiency to meet the challenge of large-scale simulations of structural systems under multi-hazard scenarios of performance-based design.

7. References

[1] Do, T. N. and Filippou F. C. (2016). A damage model for structures with degrading response. *Submitted for publication to Earthquake Engineering & Structural Dynamics*

[2] FEMA (2009). Effects of strength and stiffness degradation on seismic response. Technical Report FEMA P-440A, Federal Emergency Management Agency, Washington, D.C.

[3] Vamvatsikos, D. and Cornell, C. A. (2002). Incremental Dynamic Analysis. *Earthquake Engineering & Structural Dynamics*, 31(3):491–514.

[4] Saatcioglu, M. and Grira, M. (1999). Confinement of reinforced concrete columns with welded reinforced grids. *Structural Journal*, 96(1):29–39.

[5] Sezen, H. and Moehle, J. (2002). Seismic behavior of shear-critical reinforced concrete building columns. In *Proceedings of the 7th US National Conference on Earthquake Engineering.*

[6] Porter, K. A. (2015). Safe enough? A building code to protect our cities as well as our lives. *Earthquake Spectra.*

[7] PEER (2010). Guidelines for performance-based seismic design of tall buildings. Technical Report 2010/05, Pacific Earthquake Engineering Research Center, Berkeley, CA.

[8] FEMA (2012). Seismic performance assessment of buildings. Volume 1–Methodology. Technical Report FEMA P-58-1, Federal Emergency Management Agency, Washington, DC.

[9] FEMA (2009). Quantification of building seismic performance factors. Technical Report FEMA P-695, Federal Emergency Management Agency, Washington, D.C.

[10] Ibarra, L. F. and Krawinkler, H. (2005). Global collapse of frame structures under seismic excitations. Pacific Earthquake Engineering Research Center.

[11] Ramirez, C. M. and Miranda, E. (2012). Significance of residual drifts in building earthquake loss estimation. *Earthquake Engineering & Structural Dynamics*, 41(11):1477–1493.